Experimental report

14/02/2019

Proposal: **5-14-263** **Council:** 4/2018

Title: Neutron diffraction study on the lattice of thermoelectric material Ag9GaSe6

Research area: Physics

This proposal is a new proposal

Main proposer: **Jie MA**

Experimental team: Qingyong REN
Jie MA

Local contacts: Jose Alberto RODRIGUEZ VELAMAZAN

Samples: Ag9GaSe6

Instrument	Requested days	Allocated days	From	To
D9	8	4	22/10/2018 25/10/2018	25/10/2018 26/10/2018

Abstract:

Thermoelectrics can directly convert heat into electricity and is considered to have potential application in energy harvesting. It is straightforward that the thermoelectric performance could be optimized by tailoring the electronic properties and suppressing the thermal conductivity, k. As an typical example, recent studies on Ag9GaSe6 demonstrated that large number of atoms in the primitive cell and weakly bonded Ag atoms endue this material a quite low thermal conductivity, and eventually a large zT. There is a phase transition at 281 K, from the low-temperature \beta-Ag9GaSe6 (P213) to the high-temperature \alpha-Ag9GaSe6 (F-43m). Except the lattice dynamics effect, theoretical calculation indicates that this system exhibits a diffusive behavior at high temperature, which makes the loose bonds of Ag atoms to neighboring atoms. Moreover, a smaller constant-volume heat capacity is reported as a solid-like material, suggesting an ionic-liquid like behavior in this compound. However, the study on the lattice in detail is still missing. We would measure the accurate details, such as the atomic position and mean-square-displacement as a function of temperature.

Ultralow lattice thermal conductivity in Ag_8SnSe_6 thermoelectric material

Qingyong Ren (2019.02.12)

1. Background

The demand for sustainable energies has motivated a great many of researches on different types of energy conversion technologies in the past decades. Thermoelectrics, which can directly convert heat into electricity, is considered to have potential application in energy harvesting. The efficiency of this energy conversion process is quantified by the thermoelectric figure of merit, $zT = \sigma S^2 T/(\kappa_{ele} + \kappa_{lat})$, where σ, S, T, κ_{ele}, and κ_{lat} are the electric conductivity, the Seebeck coefficient, the absolute temperature, and the electronic and lattice contributions to the thermal conductivity, respectively [1]. It is straightforward from this formula that the thermoelectric performance could be optimized by tailoring the electronic properties (electronic conductivity and Seebeck coefficient), and by suppressing the thermal conductivity, κ ($=\kappa_{ele} + \kappa_{lat}$), as much as possible. σ, S, and κ_{ele} strongly couple with each other, and this make it difficult to improve zT through tune these three parameters. Alternatively, suppressing κ_{lat} is an important and effective strategy [2, 3]. The lattice thermal conductivity can be described by $\kappa_{lat} = 1/3cv^2\tau = 1/3cvl$,where c, v, τ and l are heat capacity, phonon velocity, phonon mean free path and phonon relaxation time, respectively [4]. κ_{lat} can be lowered by suppressing any of these three parameters.

Recently, the argyrodite-type $A_{(12-n)/m}^{m+}B^{n+}X_6^{2-}$ compounds ($A^{m+} = Li^+$, Cu^+, or Ag^+, $B^{n+} = Ga^{3+}$, Si^{4+}, Ge^{4+}, Sn^{4+}, P^{5+}, or As^{5+}, and X = S, Se, or Te) have received a great many of attentions as a group of promising thermoelectric materials with ultralow lattice thermal conductivities [5-11]. One possible reason for the ultralow lattice thermal conductivity in argyrodite-type materials is the large unit cell with complex structure and weak chemical bonds [10, 11]. The weakly-bonded Ag^+ cations with heavy atomic mass lead to low phonon group velocities. In addition, large and complex unit cell would fold back the high-frequency portions of acoustic phonon branches and lower the cutoff frequency of the acoustic phonons. In other words, population of the acoustic phonon branches, which have higher group velocity than optical phonon branches and play main role in heat conduction, in samples with large and complex unit cell is intrinsically smaller than other samples with relatively smaller unit cell. Such reduction of acoustic phonon population are responsible for the low thermal conductivity.

One alternative explanation is that the argyrodite-type samples exhibits liquid-like superionic behavior [8, 9]. As a typical example, Ag_8SnSe_6 exhibit a phase transition from the low-temperature β-Ag_8SnSe_6 (space group *Pmn2₁*) to the high-temperature γ-Ag_8SnSe_6 (space group *F-43m*) [12, 13]. Above the transition temperature, the Ag^+ cations distribute at three different atomic positions. The non-fully-occupied states of Ag^+ allow it jump between different sites. This diffusive behavior of Ag^+ in the $SnSe_6$-sublattice would damp the transverse phonon vibration. One macroscopic evidence is the smaller constant-volume heat capacity C_v than $3Nk_B$ for 3-dimensional solid-like materials, similar to Cu_2Se [6]. However, Voneshen et al. argue that the diffusion process of Cu^{2+} is too slow to interfere the transverse phonon propagation. They attribute the ultralow lattice thermal conductivity rather to strong anharmonic vibration of the Cu^{2+} [14].

Neutron scattering techniques demonstrate a powerful capacity in the study of harmonic/anharmonic lattice vibrations as well as liquid-like superionic behaviors. To unveil the underlying mechanisms that engender an ultralow lattice thermal conductivity in Ag_8SnSe_6, we designed to take neutron single crystal diffraction (for average structure) and quasi-elastic neutron scattering (QENS, for diffusive behaviors) measurements.

2. Experimental details

In this project, single crystal neutron diffraction experiments were carried out using the Hot Neutron 4-circle Diffractometer (D9) at the Institut Laue-Langevin. The sample was measured at two different temperature points, 400 K and 650 K, above the phase transition. The data was analyzed using integrated intensity refinement method [15, 16] and maximum entropy method (MEM) [17, 18].

3. Results and analysis

According to the XRD pattern as shown in Fig. 1(a), the sample can be identified as the β-Ag_8SnSe_6 phase with a space group of $Pmn2_1$ at room temperature. Fig. 1(c,e) shows the crystal structure and the neutron scattering-length densities determined by integrated intensity refinement and MEM analysis of neutron diffraction data at 400 K and 650 K, respectively. The sample crystallize into a cubic structure with *F-43m*. The crystal details are summarized in Table 1. The neutron scattering-length densities projected along the <111> directions are shown in Fig. 1(d,f). Both contour image demonstrated a localized diffusion of Ag^+ cations between the two 48*h* position, and this is consistent with the dramatic enhancement of their atomic displacement parameters with temperature. However, the diffusive route does not connected across the unit cell, indicating that this compound might just be a quasi-superionic material. Bond-valence energy landscapes calculation will be done, which will give a clear map of diffusive route from the aspect of energy.

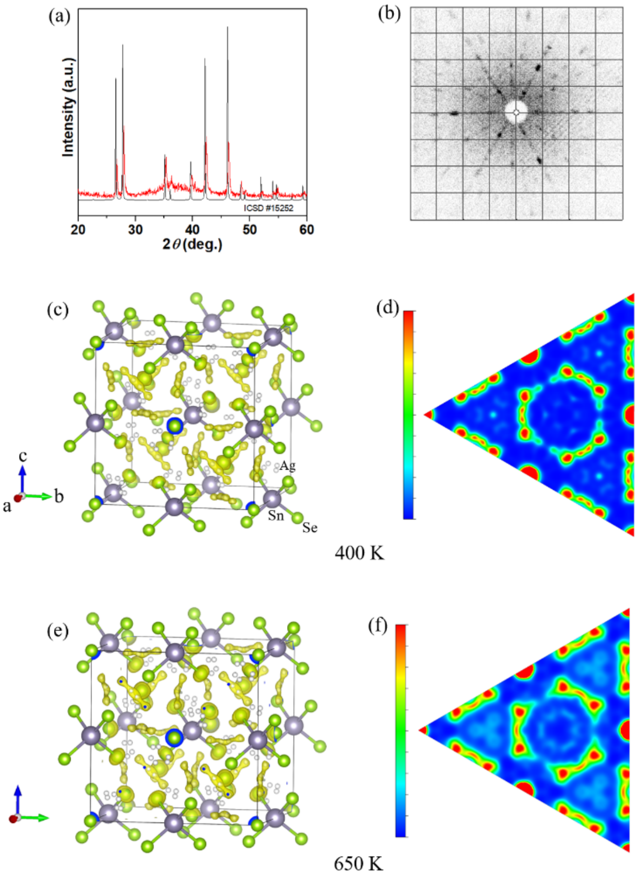

Fig. 1 (a) XRD diffraction pattern for Ag_8SnSe_6 powder sample with cubic structure (*F-43m*). (b) Laue diffraction of the Ag_8SnSe_6 crystal on the (010) plane. Isosurfaces (2% of maximum density) of the neutron scattering-length densities determined by maximum entropy analysis of neutron diffraction data and corresponding projection along [111] at (c,d) 400 K and (e,f) 650 K

Table 1. Refined parameters and crystallographic details from the integrated intensity refinement of the neutron diffraction data of Ag_8SnSe_6 at different temperatures.

Atom	site	Symmetry	*x*	*y*	*z*	U_{11}	U_{22}	U_{33}	U_{12}	U_{13}	U_{23}	Occupancy
Temperature: 400 K Space group: *F-43m* Unit cell a (Å): 11.1375 Density (g/cm3): 6.683 Goodness-of-fit:												
Sn1	*4b*	*-43m*	0.5	0.5	0.5	0.0226(11)	0.0226(11)	0.0226(11)	0	0	0	1
Se1	*4a*	*-43m*	0	0	0	0.104(4)	0.104(4)	0.104(4)	0	0	0	1
Se2	*4c*	*-43m*	0.25	0.25	0.25	0.072(3)	0.072(3)	0.072(3)	0	0	0	1
Se3	*16e*	*.3m*	0.62991(13)	0.62991(13)	0.62991(13)	0.0318(7)	0.0318(7)	0.0318(7)	-0.0076(6)	-0.0076(6)	-0.0076(6)	1
Ag1	*96i*	*1*	-0.155(6)	0.056(5)	0.129(5)	0.10(2)	0.10(2)	0.10(2)	0	0	0	0.062(12)
Ag2	*48h*	*..m*	-0.1735(11)	-0.1735(11)	0.0231(16)	0.085(9)	0.085(9)	0.085(9)	0	0	0	0.28(2)
Ag3	*48h*	*..m*	0.2295(8)	0.2295(8)	0.0359(10)	0.053(5)	0.053(5)	0.053(5)	0	0	0	0.214(14)
Temperature: 650 K Space group: *F-43m* Unit cell a (Å): 11.2019 Density (g/cm3): 6.866 Goodness-of-fit: 3.04												
Sn1	*4b*	*-43m*	0.5	0.5	0.5	0.0378(14)	0.0378(14)	0.0378(14)	0	0	0	1
Se1	*4a*	*-43m*	0	0	0	0.093(3)	0.093(3)	0.093(3)	0	0	0	1
Se2	*4c*	*-43m*	0.25	0.25	0.25	0.078(3)	0.078(3)	0.078(3)	0	0	0	1
Se3	*16e*	*.3m*	0.62957(15)	0.62957(15)	0.62957(15)	0.0511(9)	0.0511(9)	0.0511(9)	-0.0136(6)	-0.0136(6)	-0.0136(6)	1
Ag1	*96i*	*1*	-0.154(6)	0.068(5)	0.127(5)	0.09(3)	0.09(3)	0.09(3)	0	0	0	0.040(8)
Ag2	*48h*	*..m*	-0.1725(15)	-0.1725(15)	0.0229(17)	0.156(9)	0.156(9)	0.156(9)	0	0	0	0.39(2)
Ag3	*48h*	*..m*	0.232(2)	0.232(2)	0.0347(16)	0.108(10)	0.108(10)	0.108(10)	0	0	0	0.195(17)

References

[1] G. J. Snyder and E. S. Toberer, *Nat Mater* **7**, 105 (2008).

[2] O. Delaire, J. Ma, K. Marty, A. F. May, M. A. McGuire, M. H. Du, D. J. Singh, A. Podlesnyak, G. Ehlers, M. D. Lumsden and B. C. Sales, *Nat Mater* **10**, 614 (2011).

[3] J. Ma, O. Delaire, A. F. May, C. E. Carlton, M. A. McGuire, L. H. VanBebber, D. L. Abernathy, G. Ehlers, T. Hong, A. Huq, W. Tian, V. M. Keppens, Y. Shao-Horn and B. C. Sales, *Nat Nanotechnol* **8**, 445 (2013).

[4] E. S. Toberer, A. Zevalkink and G. J. Snyder, *Journal of Materials Chemistry* **21**, 15843 (2011).

[5] W. F. Kuhs, R. Nitsche and K. Scheunemann, *Materials Research Bulletin* **14**, 241 (1979).

[6] L. Li, Y. Liu, J. Dai, A. Hong, M. Zeng, Z. Yan, J. Xu, D. Zhang, D. Shan, S. Liu, Z. Ren and J.-M. Liu, *J. Mater. Chem. C* **4**, 5806 (2016).

[7] W. Li, S. Lin, B. Ge, J. Yang, W. Zhang and Y. Pei, *Adv Sci (Weinh)* **3**, 1600196 (2016).

[8] B. Jiang, P. Qiu, H. Chen, Q. Zhang, K. Zhao, D. Ren, X. Shi and L. Chen, *Chem Commun* **53**, 11658 (2017).

[9] B. Jiang, P. Qiu, E. Eikeland, H. Chen, Q. Song, D. Ren, T. Zhang, J. Yang, B. B. Iversen, X. Shi and L. Chen, *J. Mater. Chem. C* **5**, 943 (2017).

[10] S. Lin, W. Li, S. Li, X. Zhang, Z. Chen, Y. Xu, Y. Chen and Y. Pei, *Joule* **1**, 816 (2017).

[11] W. Li, S. Lin, M. Weiss, Z. Chen, J. Li, Y. Xu, W. G. Zeier and Y. Pei, *Advanced Energy Materials*, 1800030 (2018).

[12] J. P. Deloume, R. Faure, H. Loiseleur and M. Roubin, *Acta Crystallographica Section B* **34**, 3189 (1978).

[13] J.-P. Deloume and R. Faure, *Journal of Solid State Chemistry* **36**, 112 (1981).

[14] D. J. Voneshen, H. C. Walker, K. Refson and J. P. Goff, *Phys Rev Lett* **118**, 145901 (2017).

[15] H. Rietveld, *J. Appl. Crystallogr.* **2**, 65 (1969).

[16] J. Rodríguez-Carvajal, *Commission on powder diffraction (IUCr). Newsletter* **26**, 12 (2001).

[17] S. M. and S. M., *Acta Crystallographica Section A* **46**, 263 (1990).

[18] K. Momma, T. Ikeda, A. A. Belik and F. Izumi, *Powder Diffr.* **28**, 184 (2013).